Input Shapers for Reducing Overshoot in Human-Operated Flexible Systems

Joshua Vaughan and William Singhose

Abstract— Input shaping is a command generation method for creating commands that result in low levels of residual vibration. The vibration reduction is accomplished by slightly increasing the acceleration and deceleration periods of the command. The increase in the deceleration period can lead to system overshoot. This paper presents a new class of Zero Overtravel (ZO) input shapers that are designed to reduce shaper-induced overtravel from human-operator commands. During the development of these new shapers, an expression for shaper-induced overtravel is introduced. This expression is used as an additional constraint in the input shaper design process to generate the ZO shapers. Experiments from a portable bridge crane verify the theoretical predictions.

I. INTRODUCTION

Input shaping generates commands that effectively reduce vibration in mechanical systems [1]–[3]. To accomplish the vibration reduction, input shaping slightly modifies the reference command by convolving it with a series of impulses called an input shaper. The input shaper is designed using estimates of the system's natural frequency and damping ratio. This process is demonstrated in Fig. 1 using a two-impulse sequence called a Zero Vibration (ZV) shaper. The figure shows a velocity pulse input and the resulting position response of a harmonic oscillator. When the pulse is properly shaped, the oscillator moves without residual vibration.

The penalty for the dramatic reduction in vibration is a slight lengthening of the command by an amount equivalent to the duration of the input shaper (typically 0.5–1.5 vibration periods). This increase in command duration not only slightly increases the rise time of the command, but also causes some system motion after the user has commanded the system to stop. This continued motion, which occurs for one shaper duration, is needed to suppress the vibration excited during the deceleration portion of the command. However, to accurately position a system, a human operator must estimate this travel distance. This effect may make precise positioning of the system difficult, especially for inexperienced operators.

This paper presents a new class of input shapers designed to decrease the stopping distance of shaped commands generated by human operators. Final positioning error will be a primary consideration for these commands. During the formulation of these new shapers, commands are assumed to be velocity commands. This is consistent with how many machines are controlled by human operators, including cranes, which are the primary application discussed in this paper.

The next section defines "overtravel" and "overshoot", as they are used in this paper. An expression of input

All authors are with The George W. Woodruff School of Mechanical Engineering, Georgia Institute of Technology, Atlanta, GA, USA `singhose@gatech.edu`
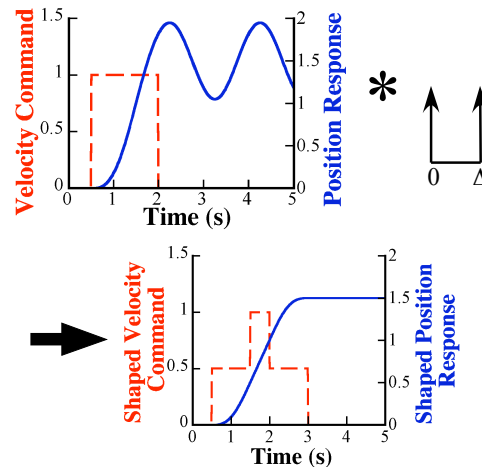
Fig 1. The Input Shaping Process

shaper overtravel is introduced in Section III. In Section IV, a constraint based on this expression is used to generate shapers that provide zero overtravel beyond the unshaped case. Finally, Section V presents experimental results from a portable bridge crane that verify the theoretical predictions.

II. OVERTRAVEL AND OVERSHOOT

All physical systems have acceleration limits that prevent instantaneous velocity changes. Therefore, velocity pulse commands are effectively changed to trapezoids, where the positive and negative steps of the pulse are changed to ramps. When trapezoidal velocities are used in conjunction with a human operator, even the unshaped command will move the system beyond where the user issues the "Stop Now" command. This effect is shown in Fig. 2, where the ramp to zero velocity takes a finite amount of time. During this time, the system will move an amount equal to the area of the hatched region in Fig. 2. As a result, all commands will have some amount of travel beyond the "Stop Now" point.

Also shown in Fig. 2 is the ZV-shaped version of the same velocity profile. It is immediately obvious that the ZV-shaped command takes longer to reach zero velocity. The distance that the input-shaped system will move after the "Stop Now" command is the sum of the hatched and shaded regions in the figure. The overtravel caused solely by the input shaper is equal to the shaded region. The area of this region is easily described using the impulse amplitudes and times of the input shaper. Furthermore, it is independent of the form of the original unshaped command (provided the unshaped command meets certain criteria).

When the commands in Fig. 2 are issued to a bridge crane, the overhead trolley responds as shown in Fig. 3.
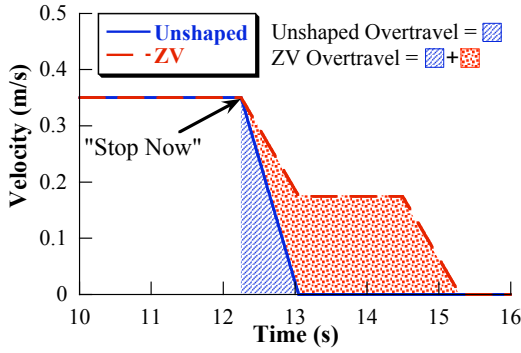
Fig 2. Overtravel During Deceleration
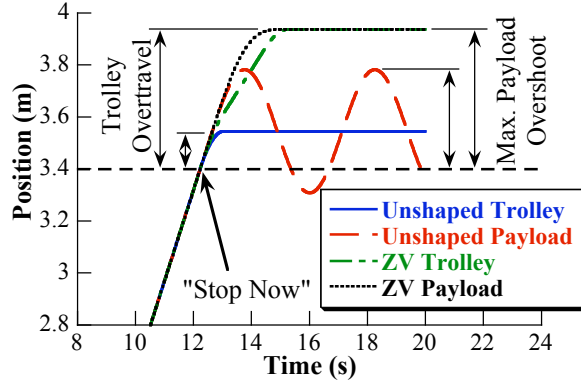
Fig 3. Overtravel and Overshoot for Unshaped and ZV-Shaped Commands

Fig 4. Diagram of Trolley Overtravel and Payload Overshoot
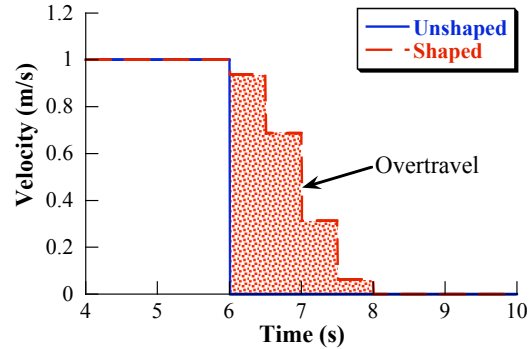
Fig 5. Shaper Overtravel Beyond the Unshaped Command

Notice both the unshaped and ZV-shaped cases result in some trolley overtravel. For the ZV-shaped case, the final positioning error is much larger. The payload responses for the two cases are also shown in Fig. 3. Notice that the unshaped command exhibits significant oscillation, resulting in overshoot that is much greater than the trolley positioning error. However, for the ZV-shaped case, the payload response exhibits no oscillation and the payload deviation from the desired position is equal to the trolley overtravel.

The difference between the trolley overtravel and the maximum overshoot of the payload from the desired position indicates the need for precise terminology. The trolley's deviation from the desired position will be called *overtravel*. The maximum deviation of the payload from the desired position will be called *overshoot*. The difference between trolley overtravel and payload overshoot is shown schematically in Fig. 4, where x_d represents the desired final position.

III. Input Shaper Overtravel and Overshoot

Given that input shapers cause overtravel and overshoot, having an expression that describes each independent of the reference command would be useful. In Fig. 5, the distance that an input-shaped command travels beyond the unshaped case is described by the shaded region of the plot. This area can be represented in terms of shaper impulse times and amplitudes. It is essentially a coarse integration of the velocity command, using the shaper impulse times as the
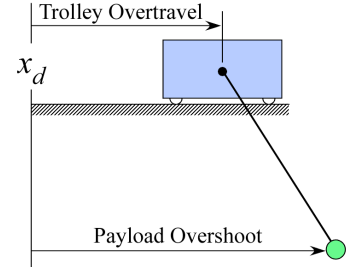
integration step size. The equation describing the area is:

$$x^+ \equiv x(t_f + t_n) - x(t_f) = V_{stop} \sum_{i=2}^{n} A_i t_i \qquad (1)$$

where n is the number of impulses in the shaper, t_f is the "stopping" time, V_{stop} is the velocity when the deceleration portion of the command begins, and A_i and t_i are the ith impulse amplitude and time location, respectively.

It is useful to describe the overtravel independent of the reference command and system parameters. To do so, (1) can be normalized by multiplying by $(V_{stop}\tau)^{-1}$, where τ is the vibration period the shaper was designed to suppress. The normalized overtravel caused solely by the input shaper is then given by:

$$\bar{x}^+ \equiv \bar{x}(t_f + t_n) - \bar{x}(t_f) = \frac{1}{\tau} \sum_{i=2}^{n} A_i t_i \qquad (2)$$

This represents the overtravel of the shaped command beyond that caused by the original reference command. The equation will hold true for all commands that meet two constraints: the unshaped and shaped commands must *i)* begin decelerating from the same velocity and *ii)* decelerate to zero velocity.

The normalized overtravel of several input shapers is [4], [5] shown in Fig. 6. To the left of the vertical line are shapers that have only positive impulses, sorted from left to right according to increasing robustness to modeling errors. As expected, the more robust, longer duration shapers produce larger amounts of overtravel. To the right of the vertical line are several common unity magnitude shapers. The impulse amplitudes in unity magnitude shapers are constrained to ±1
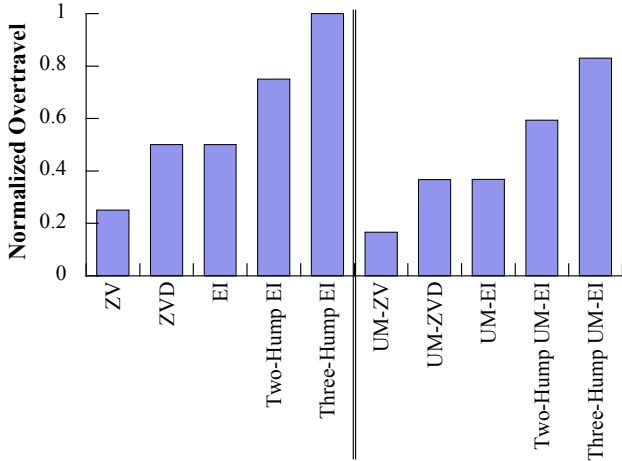
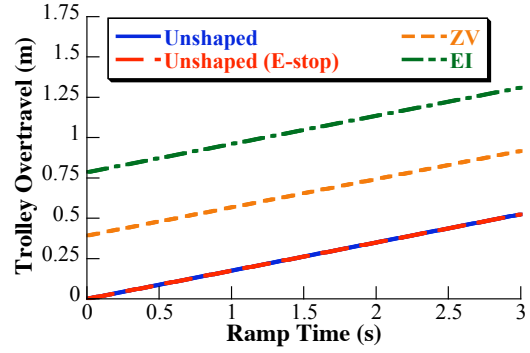**Fig 6. Normalized Overtravel of Common Shapers**

[6], [7]. Again, the more robust, longer duration shapers produce larger amounts of overtravel. However, the overtravel induced by the shorter-duration unity magnitude shapers is less than with their positive counterparts.

To better understand what these values of normalized overtravel mean, simulations of a typical industrial bridge crane were performed. In the simulations, the suspension cable length was set to 5m and the maximum velocity to $0.35 \frac{m}{s}$. To test a range of ramp-times, simulations were conducted using ramp-times ranging from 0.0s to 3.0s. For all cases, the command duration was chosen to be long enough that the trolley reached its maximum velocity before deceleration began.
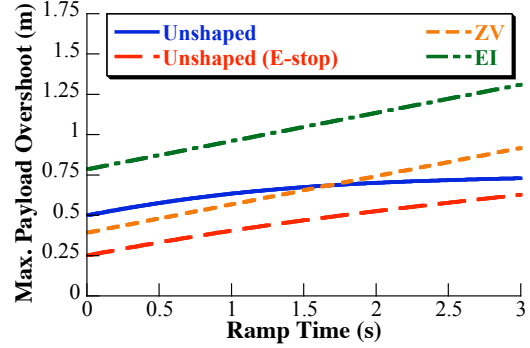
Figure 7(a) shows the trolley overtravel as a function of ramp-time for two unshaped commands and commands shaped by ZV [1], [2] and EI [8], [9] input shapers. In the first unshaped case, the command is completely unshaped; the acceleration and deceleration portions of the command both caused payload oscillation. In the second case, labeled *Unshaped (E-stop)*, the acceleration portion of the command was input shaped so that it reached maximum velocity without payload oscillation. For the deceleration phase, input shaping was not used. This mimics an "E-stop" condition, where the crane is forced to stop as quickly as possible.

The ZV- and EI-shaped commands display larger amounts of trolley overtravel than the unshaped cases at all values of ramp time. This is expected given the results shown in Fig. 6. It is also important to note that the overtravel of the shaped commands increases at the same rate as the unshaped commands (*i.e.*, the slopes are the same). The overtravel caused solely by input shaping remains constant. This confirms the prediction given in (2).

Figure 7(b) shows the corresponding maximum payload overshoot. Both unshaped cases exhibit much more payload overshoot than trolley overtravel. The maximum payload overshoot and trolley overtravel are nearly equal for the shaped commands. This is because each shaped command excited only a small amount of vibration. The final point to notice is that for ramp times below 1.5s, the maximum payload overshoot for the ZV shaped command is less than that of the unshaped command. This is an important point;

(a) Trolley Overtravel

(b) Maximum Payload Overshoot

Fig 7. Overtravel and Overshoot as a Function of Ramp Time

even if the trolley overtravels farther than the unshaped case, the payload does not.

IV. ZERO OVERTRAVEL (ZO) SHAPERS

The normalized overtravel equation, (2), can be used as a design constraint on the shaper-induced overtravel:

$$\bar{x}^+ \equiv \frac{1}{\tau} \sum_{i=2}^{n} A_i t_i \leq \bar{x}^+_{des} \qquad (3)$$

where $\bar{x}^+_{des}$ is the desired amount of shaper-induced overtravel. This constraint can be used in conjunction with any desired vibration constraints. It is important to note, however, that to reduce the amount of shaper-induced overtravel, negative impulses must be allowed. Because negative impulses are needed, higher amounts of high-mode excitation can occur [10]. The following sections will present several classes of input shapers developed using this constraint.

A. Zero Vibration–Zero Overtravel (ZV-ZO) Shapers

Zero Vibration–Zero Overtravel (ZV-ZO) shapers seek to limit both residual vibration and shaper-induced overtravel to zero. The residual vibration constraints are identical to the ZV shaper. The zero overtravel constraint is:

$$\frac{1}{\tau} \sum_{i=2}^{n} A_i t_i = 0 \qquad (4)$$

In addition to the zero vibration and zero overtravel constraints, impulse amplitudes are constrained between negative

TABLE I. ZV-ZO Shapers for Damped Systems

$$t_i = (M_0 + M_1\zeta + M_2\zeta^2)\tau, \quad \tau = \frac{2\pi}{\omega}$$

$$A_i = M_0 + M_1\zeta + M_2\zeta^2$$

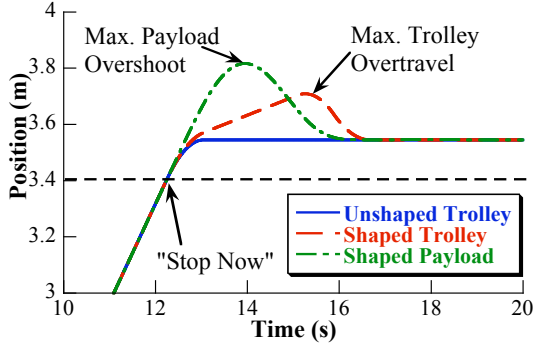|	M_0	M_1	M_2
A_1	0.8170	0.6871	-0.7456
A_2	1.0000	0.0000	0.0000
A_3 (= -A_1)	-0.8170	-0.6871	0.7456
t_2	0.6457	0.3982	0.2244
t_3	0.7898	-0.1504	0.8577

Fig 8. Simulation Responses to Unshaped and ZV-ZO Velocity Profiles

one and positive one:

$$-1 \le A_i \le 1, \quad i = 1, \ldots, n \quad (5)$$

One difference between this constraint and unity magnitude [6] or specified negative amplitude impulse amplitude constraints [10], [11] is that the sign of the impulses is not forced to alternate. Impulse amplitudes are also constrained to sum to one. Given the nonlinearity of the constraint set for the ZV-ZO shapers, impulse amplitudes and times are determined using a numerical solver.

The ZV-ZO shaper for undamped systems is:

$$\begin{bmatrix} A_i \\ t_i \end{bmatrix} = \begin{bmatrix} 0.8164 & 1.000 & -0.8164 \\ 0 & 0.6451\tau & 0.7902\tau \end{bmatrix} \quad (6)$$

For systems with viscous damping, the amplitudes and times become functions of the damping ratio, as shown in Table I. The shapers described in Table I are the result of curve fits for a series of solutions over the range $0 \le \zeta \le 0.3$. The maximum error of the fit for any impulse time or amplitude is less that 0.05% in the range.

When using Zero Overtravel shapers, a standard input shaper should be used to shape the acceleration portion of the command. The ZO shaper should only be used on the deceleration portion of the command. Using a ZO shaper on the acceleration portion of the velocity pulse can create a command with a higher maximum velocity than the unshaped command. The shaped deceleration command will have a region of negative velocity so that the zero overshoot constraint can be achieved.

Figure 8 shows the simulated response of the bridge crane to unshaped and ZV-ZO shaped trapezoidal velocity profiles. The trolley and payload responses to the ZV-ZO command both have brief periods of travel beyond the final, steady-state position. Because the constraint on overshoot given in (4) represents the travel of a shaped command beyond an
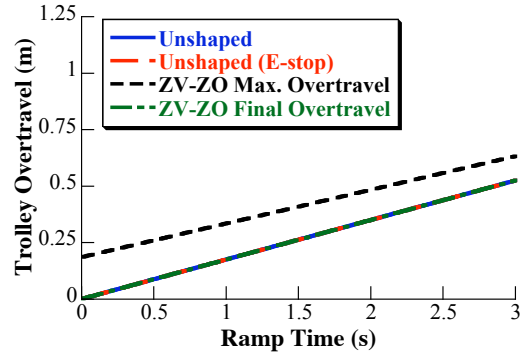
(a) Trolley Overtravel
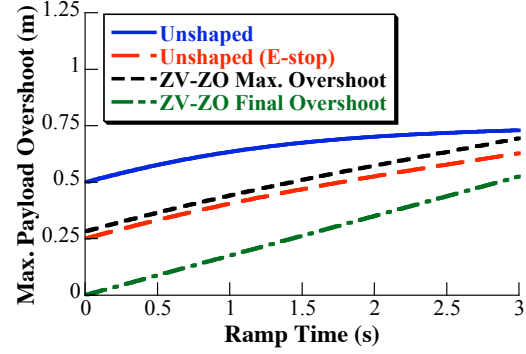
(b) Payload Overshoot

Fig 9. Overtravel and Overshoot as a Function of Ramp Time for Unshaped and ZV-ZO Shaped Commands

unshaped command, the trolley and payload do not return to the desired final position. Instead, they return to the final position of the unshaped command.

Figures 9(a) and 9(b) show the trolley overtravel and payload overshoot using the ZV-ZO shaper over a range of trapezoidal velocity ramp times. For all ramp times shown, the final overtravel of the trolley using the ZV-ZO shaped command is identical to that of the unshaped command. This is the same value of final payload overshoot shown in Fig. 9(b); the payload reaches the same final position as the trolley, with no vibration. Also shown in Fig. 9(b) is the maximum payload overshoot for the ZV-ZO shaper. This value remains below the unshaped overshoot for all values shown. The ZV-ZO shaper not only returns the trolley to the same position as the unshaped command, it does so with less payload deviation from the desired final position.

Input shaper robustness is typically shown via the sensitivity curve, which indicates how much vibration will occur as system parameters change. The frequency sensitivity curve for the ZV-ZO shaper is shown in Fig. 10. Insensitivity is the width of the sensitivity curve below the tolerable level of vibration [8], [9]. The price for the zero overtravel constraint of the ZV-ZO shaper is shown in the plot; the shaper's Insensitivity at a $V_{tol} = 5\%$, I(5%), is 0.03. This is half that of the standard ZV shaper, which has I(5%) of 0.06.

B. Specified Insensitivity–Zero Overtravel (SI-ZO) Shapers

Given the low robustness of the ZV-ZO shaper, it is clear that more robust zero overtravel shapers are necessary.
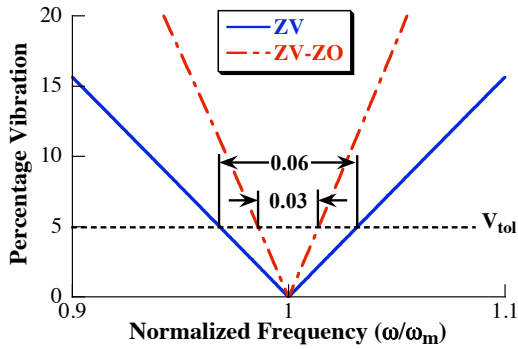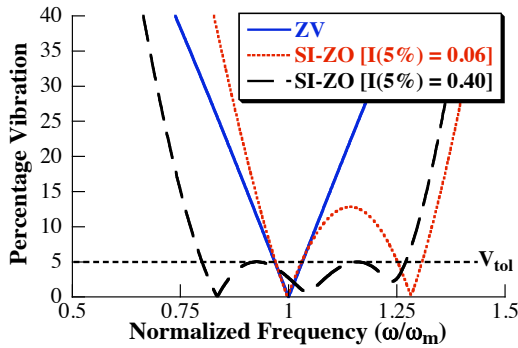
Fig 10. ZV-ZO Shaper Sensitivity Curve

Fig 11. Sensitivity Curves of two SI-ZO shapers

If the zero overtravel constraint from (4) and the impulse amplitude constraints from Section IV-A are combined with Specified Insensitivity vibration constraints [12], [13], then SI-ZO shapers result. These shapers allow the Insensitivity to be set to any value, while maintaining zero final overtravel.

For example, the sensitivity curve of an SI-ZO shaper designed to have the same 5% Insensitivity as a standard ZV shaper (I(5%) = 0.06) is shown by the dotted line in Fig. 11. More robust SI-ZO shapers are also possible. For example, Fig. 11 also shows the sensitivity curve of a SI-ZO shaper with the same 5% Insensitivity as an EI shaper (I(5%) = 0.40). Figure 12 shows the payload responses resulting from the SI-ZO shapers described in Fig. 11. Notice that maximum payload overshoot for SI-ZO [I(5%) = 0.40] is larger than for the SI-ZO [I(5%) = 0.06] shaper.
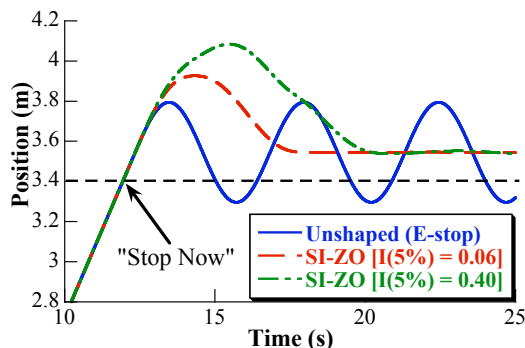
There are a few penalties for achieving robust zero over-

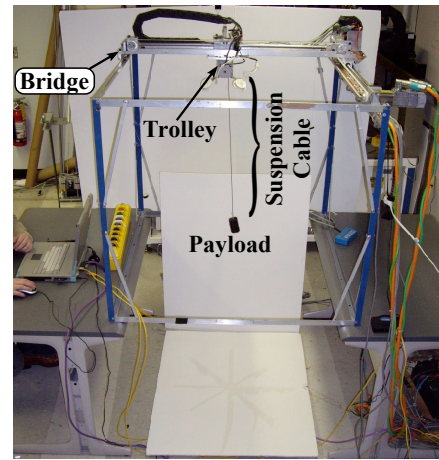**Fig 12. Payload Response to SI-ZO Commands**

Fig 13. Portable Bridge Crane

travel. The first is that the shaper contains a larger number of impulses and is longer in duration than the ZV-ZO shaper. The second is that the maximum amount of overtravel and overshoot increases with robustness.

V. EXPERIMENTAL VERIFICATION OF ZERO OVERSHOOT INPUT SHAPERS

To test the effectiveness of the zero overtravel input shapers on a real machine, experiments were conducted on the portable bridge crane shown in Fig. 13 [14]. The portable bridge crane has a workspace of approximately 1m×1m×1.6m. The overhead bridge and trolley are driven using Siemens synchronous AC servomotors attached to timing belts, controlled using a Siemens PLC. An overhead vision system can measure payload position.

Commands were generated to move the trolley approximately 0.38m, if no overtravel occurred. Deceleration ramp times were varied between 0.2s and 1.2s at intervals of 0.2s. However, to accommodate the small workspace of the portable bridge crane, the acceleration ramp time was held constant at 0.2s. In addition, for all cases but the unshaped, the acceleration portion of the command was shaped with a ZV shaper. This ensured very little vibration at the beginning of the deceleration phase.

Figure 14 shows the maximum payload overshoot resulting from unshaped and unshaped (E-stop) commands. Also shown on the plot is the theoretical trolley overtravel resulting from unshaped commands. The experimental results of payload overshoot closely match the theoretical predictions. In each case the maximum payload overshoot is greater than the trolley overtravel. This matches the predictions from the industrial bridge crane simulations in Section III.

The theoretical and experimental trolley overtravel for the SI-ZO shaper with I(5%)=0.06 are shown in Fig. 15(a). For both the maximum and final trolley overtravel, the experimental results closely align with the theoretical. The final overtravel is also equivalent to that of the unshaped case shown in Fig. 14, indicating that the zero-overtravel constraint is satisfied.
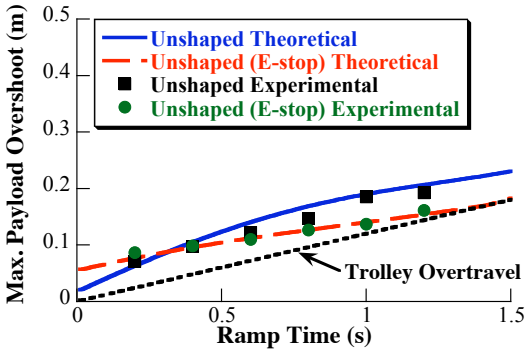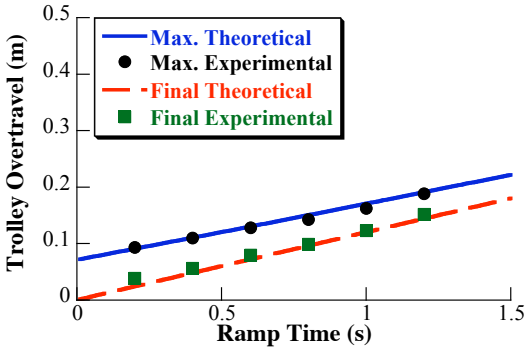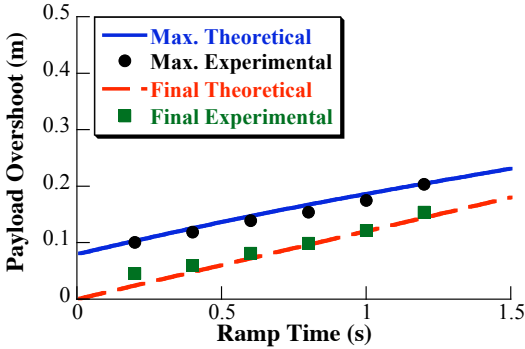
182

Fig 14. Experimental Payload Overshoot for Unshaped Commands

(a) Trolley Overtravel for SI-ZO [I(5%) =0.06] Commands

(b) Payload Overshoot for SI-ZO [I(5%) =0.06] Commands

Fig 15. Experimental Overtravel and Overshoot

The payload overshoot for the SI-ZO shaper is shown in Fig. 15(b). The experimental results closely match the theoretical prediction, providing less final payload overshoot than the unshaped cases for all ramp times. The maximum payload overshoot is also shown on the plot. Above ramp times of 0.6s, this value closely matches the maximum payload overshoot of the unshaped case.

VI. CONCLUSIONS

This paper provided an analysis of overtravel and overshoot for input-shaped commands. Using a simulation of an industrial bridge crane, the trolley overtravel and payload overshoot were presented for several common input shapers and unshaped commands. In addition, an expression describing the amount of overtravel beyond the unshaped command caused by an input shaper was given. This expression led to

an additional constraint that can be included in input shaper design. The inclusion of this constraint led to Zero Overtravel (ZO) shapers that provide the same overtravel as unshaped commands. In addition, due to the low vibration properties of the input shapers, the final payload overshoot was less than the unshaped case. Experimental results from a portable bridge crane verified the theoretical predictions.

REFERENCES

[1] O. J. M. Smith, "Posicast control of damped oscillatory systems," *Proceedings of the IRE*, vol. 45, pp. 1249–1255, September 1957.

[2] N. C. Singer and W. P. Seering, "Preshaping command inputs to reduce system vibration," *Journal of Dynamic Systems, Measurement, and Control*, vol. 112, pp. 76–82, March 1990.

[3] S. P. Bhat and D. K. Miu, "Precise point-to-point positioning control of flexible structures," *Journal of Dynamic Systems, Measurement, and Control*, vol. 112, no. 4, pp. 667–674, 1990.

[4] J. Vaughan, A. Yano, and W. Singhose, "Comparison of robust input shapers," *Journal of Sound and Vibration*, vol. 315, no. 4-5, pp. 797 – 815, 2008.

[5] ——, "Robust negative input shapers for vibration supressions," *In Press: Journal of Dynamic Systems, Measurement, and Control*, 2009.

[6] W. Singhose, N. Singer, and W. Seering, "Time-optimal negative input shapers," *J. of Dynamic Systems, Measurement, and Control*, vol. 119, pp. 198–205, June 1997.

[7] S. S. Gurleyuk, "Optimal unity-magnitude input shaper duration analysis," *Archive of Applied Mechanics*, vol. 77, no. 1, pp. 63 – 71, 2007.

[8] W. Singhose, W. Seering, and N. Singer, "Residual vibration reduction using vector diagrams to generate shaped inputs," *ASME J. of Mechanical Design*, vol. 116, pp. 654–659, June 1994.

[9] U. H. Park, J. W. Lee, B. D. Lim, and Y. G. Sung, "Design and sensitivity analysis of an input shaping filter in the z-plane," *Journal of Sound and Vibration*, vol. 243, no. 1, pp. 157–171, 2001.

[10] W. Singhose, E. Biediger, Y.-H. Chen, and B. Mills, "Reference command shaping using specified-negative-amplitude input shapers for vibration reduction," *ASME J. of Dynamic Systems, Measurement, and Controls*, vol. 126, pp. 210–214, March 2004.

[11] J. Vaughan, A. Yano, and W. Singhose, "Performance comparison of robust negative input shappers," in *2008 American Controls Conference*, Seattle, Washington, June 2008, pp. 3257 – 62.

[12] W. Singhose, W. Seering, and N. Singer, "Input shaping for vibration reduction with specified insensitivity to modeling errors," in *Japan-USA Sym. on Flexible Automation*, vol. 1, Boston, MA, 1996, pp. 307–13.

[13] W. Singhose, D. Kim, and M. Kenison, "Input shaping control of double-pendulum bridge crane oscillations," *Journal of Dynamic Systems, Measurement, and Control*, vol. 130, no. 3, pp. 1 – 7, May 2008.

[14] J. Lawrence and W. Singhose, "Design of a minicrane for education and research," in *6th Int. Conference on Research and Education in Mechatronics*, Annecy, France, 2005.